

## Supplementary Information

### Computational studies on interparticle forces between nanoellipsoids

Weifu Sun,<sup>a,\*</sup>† Qinghua Zeng,<sup>b</sup> Aibing Yu<sup>a,c,\*</sup>

<sup>a</sup>Laboratory for Simulation and Modeling of Particulate Systems, School of Materials Science and Engineering, The University of New South Wales, Sydney, NSW 2052, Australia

<sup>b</sup>School of Computing, Engineering and Mathematics, University of Western Sydney, Penrith, NSW 2751, Australia

<sup>c</sup>Department of Chemical Engineering, Monash University, Clayton, Victoria 3800, Australia

#### 1. Simulations of two closely interacting Si nanoellipsoids

Two identical silicon nanoellipsoids are closely put together at the initial surface separation apart of  $d_0=0.5 \text{ \AA}$ . After geometrical optimization, MD simulation is conducted for at least 50.0 ps using a NVT ensemble at 300 K to fully relax structure. As observed from Figure S-1, with the increase of the simulation time from 0 to 20 ps, the two nanoellipsoids becomes increasingly close to each other and the surface separation distance becomes narrower. The two nanoparticles almost intimately contact each other after 30 ps (Figure S-1d). The results show that even the surface separation is pretty close, still no surface diffusion happened. This may be because different from the dangling bonds (the coordination number equals to 1), the coordination number of the unsaturated silicon atoms on the surface of particle is still two or three, thus limiting their flexibility to move.

---

\*Corresponding author. E-mail address: aibing.yu@monash.edu (A. B. Yu). Phone: +61-3-9905-0582. Fax: +61-3-9905-5686; weifu.sun518@gmail.com, weifu.sun@sydney.edu.au (W. F. Sun)

†Current address. School of Aerospace, Mechanical and Mechatronic Engineering, The University of Sydney, NSW 2006, Australia.

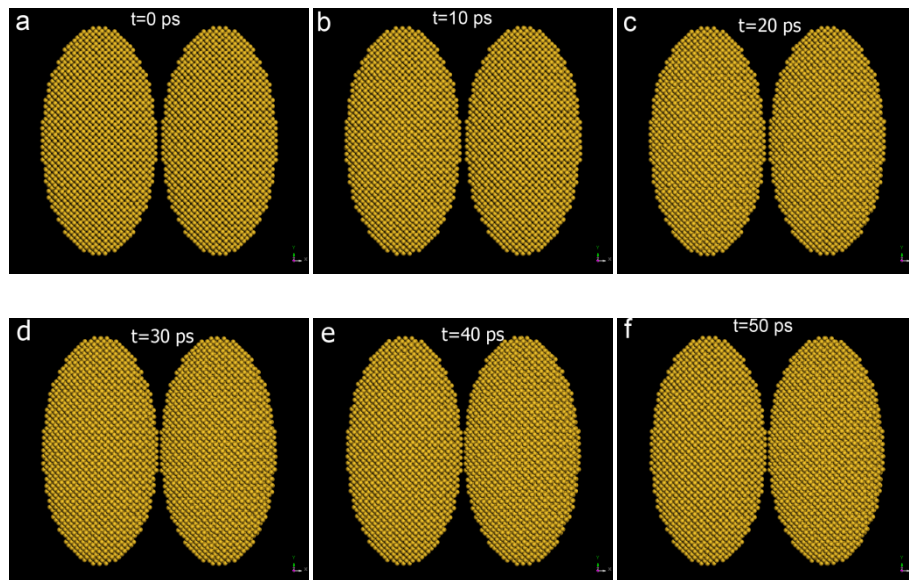


**Figure S-1.** Sequential snapshots of two closely interacting silicon nanoellipsoids of (2.5 nm, 5.0 nm, 2.0 nm) at (a) 0 ps, (b) 10 ps, (c) 20 ps, (d) 30 ps, (e) 40 and 50 ps. The initial surface separation between them is  $d_0=0.5 \text{ \AA}$ .

## 2. Characterization of Atomic Structures of Si Nanospheres

For ellipsoidal particle, there are three principal radii along the three different directions. When calculating the surface separation, to be consistent with the previous work, the principal radius along one particular direction can still be defined as done before<sup>1</sup>. The defined principal radius along one particular direction can be obtained based on the corresponding nanospheres with radius equal to the principal radius.

Since the thermal vibrations of surface atoms in nanospheres may fluctuate out of the cut-off radius  $R_0$  and the size of nanospheres becomes vague.<sup>2</sup> Therefore, the structure of Si nanospheres will be characterized following the approach proposed by Van Hoang: atoms on the surface of a nanosphere with unsaturated coordination are considered as surface atoms while those in the core with full coordination are considered as core atoms.<sup>3</sup> The definition of each parameters including their core radius  $R^{\text{core}}$ , surface roughness (rms), particle radius ( $R$ ), effective surface thickness  $\delta$  and maximum surface thickness  $\delta_{\text{Max}}$  can be found in the work<sup>1</sup> and an illustration is drawn for the convenience

of understanding (Figure S-2). By analyzing the equilibrated structure of nanospheres from the MD simulations, each parameter can be quantified and listed in Table S-1. Note that in the treatment, atoms which are not in the core are referred to as “surface atoms” while those in the core are termed as “core atoms”, and their radial distances from the nanosphere centre are denoted as  $R_i^{\text{surf}}$  or  $R_j^{\text{core}}$ , respectively.

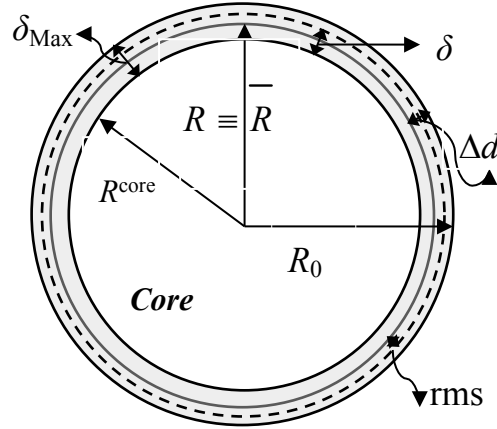


**Figure S-2.** A schematic structure of crystalline Si nanosphere with defined parameters. The shadow represents the particle surface with certain thickness.

**Table S-1** Structural parameters of Si nanospheres (Å)

$R_0$	12.5	25.0	37.5	50.0
$R^{\text{core}}$	10.8	22.7	35.0	47.5
$R$	11.56	23.68	36.04	48.49
rms	0.588	0.615	0.614	0.651
rms/ $R$	0.0508	0.0259	0.0170	0.0134
$\delta$	1.35	1.59	1.65	1.64
$\delta_{\text{Max}}$	1.46	2.17	2.26	2.45

### 3. Interplay between LJ force and mechanical contact force

Figure S-3 demonstrates the interparticle LJ potential  $E_{LJ}$ , LJ force  $F_{LJ}$ , the contact force  $F_c$  as a function of surface separation distance  $d$ . It is clear that the LJ potential first decreases to a first minimum at  $d \approx 0.14$  nm, and then increases sharply by decreasing surface separation, finally reaches a second potential minimum. By differentiating interparticle LJ potential with respect to surface separation, the as-obtained LJ force also first decreases to a first minimum, followed by increasing sharply, finally reaches a second minimum force. The first minimum point of LJ potential corresponds to the first almost zero point of LJ force at  $d \approx 0.14$  nm where the occurrence of mechanical contact force initiates, confirming that due to the intermolecular repulsive forces, the mechanical contact force arises when two surfaces are less than equilibrium separation distance apart. In addition, the twice appeared minima indicate the stepped atomic structure at the interface of two closely interacting nanoellipsoids.

As observed from Figure S-3b, the pull-off force of two parallel silicon nanoellipsoids with  $R_e = 2.5$  nm (Table 2), *i.e.*, the first minimum point, is about -2.0 nN. In view of the Hamaker constants of silica<sup>1</sup> ( $A_{\text{Silica}} = 6.5 \times 10^{-20}$  J) and  $A_{\text{Si}} = 14.8 \times 10^{-20}$  J, the pull-off force between two 40 nm-radius silica is about  $-13.2 \pm 2.6$  nN.<sup>4</sup> But considering the size difference of  $R_e = 2.5$  nm and  $R = 40$  nm and also the difference in Hamaker coefficient, the magnitude of pull-off force obtained in this work is reasonable.

In addition, it should be noted that before particle's contact, the interparticle force is dominated by LJ force while there is almost no contact force. But after contact deformation, apart from the contribution of LJ force, contact force also arises and in particular, the mechanical contact force becomes dominant: the magnitude of LJ force is far less than mechanical contact force as observed from Figure S-3b and c. Of note, our formulas can reasonably reproduce the MD simulated results before particle's contact deformation.

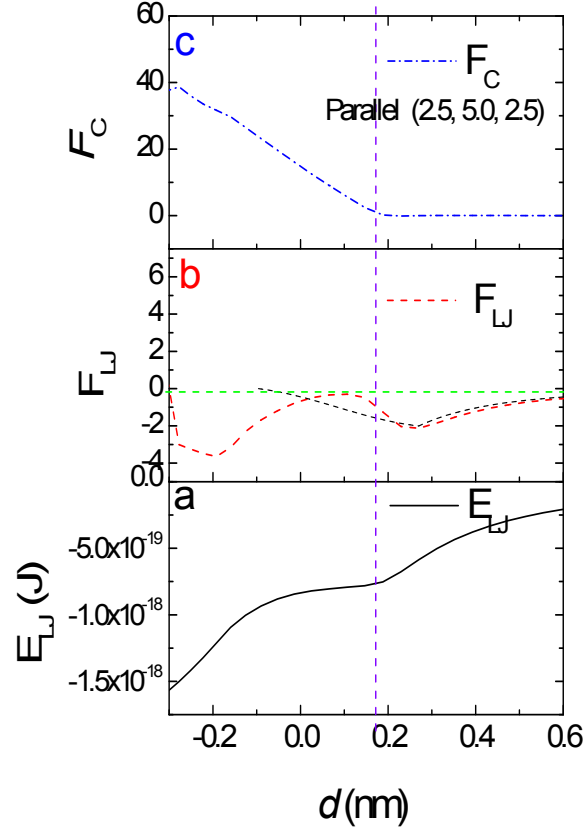


**Figure S-3.** The interplay between interparticle LJ potentials  $E_{LJ}$  (a), LJ forces  $F_{LJ}$  (b) and mechanical contact forces  $F_c$  (c) between two parallel silicon nanoellipsoids of (2.50, 5.00, 2.50) nm in radius as a function of surface separation. (b): the red dashed line represents MD simulated results while the black dashed line denotes the results calculated from our formulas of Eqs. (6) and (7).

#### 4. Supplementary nomenclature

**Table S-2** Nomenclature for symbols used in this work

Symbol	
$A$	Hamaker constant
$C$	the vdW attraction interaction parameter
$\varepsilon$	the potential well depth or strain
$\sigma$	the collision diameter of atom

$E_{LJ}$	interparticle Lennard-Jones potential
$E$	Young's modulus
$E^*$	the reduced Young's modulus
$R_0$	the cut-off radius
$R$	the defined particle radius $R = \bar{R}$
$\bar{R}$	the averaged radial distance of surface atoms from particle's centre
$R^{\text{core}}$	the radius of particle's core
$R_e$	the equivalent radius
$\chi_{12} \eta_{12}$	the orientation term
$R_1'$	the radius of principal curvature
$R_1''$	the radius of principal curvature
$\sqrt{B/A}$	aspect ratio
$F_2$	the correction factor for the eccentricity of the ellipse
$\delta$	effective surface thickness
$\delta_{\text{Max}}$	the maximum surface thickness
$\delta_n$	normal displacement
$d$	the shortest surface separation along the line of two particles' centres
$d_{\text{min}}$	The minimum surface separation
$v$	velocity or volume of atom
$\lambda$	the ratio of the particle radii of two particles
$\mathbf{F}_n$	total normal force
$\mathbf{F}_{\text{vdW}}$	van der Waals attraction force
$\mathbf{F}_{\text{Born}}$	the short range Born repulsion force

**Notes and references**

- 1 W. F. Sun, Q. H. Zeng and A. B. Yu, *Langmuir*, **2013**, *29*, 2175-2184.
- 2 S. F. Cheng and M. O. Robbins, *Tribol. Lett.*, **2010**, *39*, 329-348.
- 3 V. Van Hoang, *J. Phys. Chem. B*, **2007**, *111*, 12649-12656.
- 4 L. F. Hakim, J. H. Blackson and A. W. Weimer, *Chem. Eng. Sci.*, **2007**, *62*, 6199-6211.